Colloid Polym Sci (2018) 296:77–88
https://doi.org/10.1007/s00396-017-4217-3

ORIGINAL CONTRIBUTION

Fundamental properties, self-assembling behavior, and their temperature and salt responsivity of ionic amphiphilic diblock copolymer having poly(*N*-isopropylacrylamide) in aqueous solution

Hideki Matsuoka[1] · **Shotaro Moriya**[1] · **Shin-ichi Yusa**[2]

Received: 4 January 2017 / Revised: 10 October 2017 / Accepted: 15 October 2017 / Published online: 12 November 2017

Abstract Molecular properties and self-assembling behavior of thermo-responsive ionic diblock copolymers, poly(*N*-isopropylacrylamide)-*b*-poly(styrenesulfonate sodium salt) (PNIPAm-*b*-PSSNa), which were precisely synthesized by reversible addition-fragmentation chain transfer (RAFT) polymerization, were systematically studied as a function of temperature and added salt concentrations. Cloud point with elevation aqueous solution temperature was found at 35~40 °C for all the block copolymers studied which have a different block length and block ratio. Cloud point decreased with increasing added salt concentration, which was identified to be the critical micelle temperature (CMT) since micelle formation was confirmed at a higher temperature. The critical micelle concentration (cmc) at 50 °C could be determined by the static light scattering technique and cmc was found to increase with increasing added salt concentration. This is behavior typical of "non-surface active" polymers although it does not obey the famous Corin-Harkins law for ionic surfactants. However, the surface tension of the solution decreased with increasing polymer concentration and the adsorption of block copolymer molecules at the water surface was directly confirmed by X-ray reflectivity and foam formation observation. Micelle size was found to increase with increasing polymer concentration by dynamic light scattering. Vesicle-like particles were found by transmission electron microscopy (TEM) observation for some block copolymers. PNIPAm-*b*-PSSNa behaves as an amphiphilic block copolymer at 50 °C and has a non-surface active nature since it has an ionic block. However, the discrepancy between the non-surface active nature of cmc behavior and surface active nature of adsorption is quite mysterious, and this might be peculiar to PNIPAm-containing block copolymers since similar behavior was not observed in other ionic amphiphilic block copolymers having a conventional hydrophobic block.

Keywords Critical micelle temperature · Poly(N-isopropylacrylamide) · Polymer Micelles

Electronic supplementary material The online version of this article (https://doi.org/10.1007/s00396-017-4217-3) contains supplementary material, which is available to authorized users.

✉ Hideki Matsuoka
matsuoka.hideki.3s@kyoto-u.ac.jp

[1] Department of Polymer Chemistry, Kyoto University, Kyoto 615-8510, Japan

[2] Graduate School of Engineering, University of Hyogo, 2167 Shosha, Himeji, Hyogo 671-2280, Japan

Introduction

The ionic amphiphilic diblock copolymer, which consists of hydrophobic and ionic blocks, shows unique properties [1]. One of the most interesting recently found is "non-surface activity"; they form polymer micelles in bulk solution but the solution does not show surface tension reduction and foam formation even by shaking [2–8]. Existence of micelles in bulk solution was confirmed by scattering techniques, and no adsorption of polymer molecules at the air/water interface was confirmed by X-ray reflectivity (XR) experiments. At a glance, this property is very strange since it is out of common sense of surfactant science; at least, a micelle is defined as a molecular assembly of "surfactant (surface active agent)" in general text. There are some requirements for ionic amphiphilic diblock copolymers to be "non-surface active"; both hydrophobic and ionic blocks should be long enough (more than degree of polymerization 30), and ionic strength should be low enough [2, 4, 7, 8]. By a systematical study, the origin

of the non-surface activity was clarified to be (1) very strong electrostatic repulsion between the water surface and ionic block by an image charge effect [9, 10] and (2) very stable polymer micelle formation in the bulk [2–8]. By these two factors, the micelle state in bulk solution is thought to be more stable than the adsorbed state at the water surface. In fact, the polymer becomes surface active by salt addition, which can be reasonably understood as a contribution of salt ions to the electrostatic shielding effect. The non-surface activity was observed for many ionic amphiphilic diblock copolymers [2–8], and also, similar properties were also observed and reported by other researchers [11–18]. Hence, "non-surface activity" is a general property although there are requirements as mentioned above. Another interesting feature of non-surface active polymers is salt concentration dependence of the critical micelle concentration (cmc): cmc *increases* with increasing added salt concentration [19]. This trend is opposed to the famous Corin-Harkins law [20] for low molecular weight ionic surfactants. Since an image charge repulsion is screened by added salt ions, the adsorbed state at the water surface becomes more stable. Hence, a polymer micelle is hard to form by salt addition.

Recently, stimuli-responsive polymers are attracting attention since they induce development of "*smart*" materials [21]. One of the most studied thermo-responsive polymers is poly(*N*-isopropylacrylamide) (PNIPAm) [22]. A lower critical solution temperature (LCST) behavior was first found in 1967 [23], and it has been duly studied by many researchers [24, 25]. LCST was found to be 31–32 °C, and it becomes hydrophilic and hydrophobic below and above LCST, respectively. Hence, the block copolymer of PNIPAm and ionic polymer should be a double hydrophilic block copolymer [26] below LCST, but it should be amphiphilic above LCST. Since these characters can be switched by a temperature change, many attempts have been made to apply PNIPAm to "schizophrenic" polymers [27, 28]. Salt-induced micellization has also been reported [29] and combination with pH responsivity examined [30, 31]. Application to fluorescence switching has also been investigated [32].

In this study, block copolymers of PNIPAm and poly(styrenesulfonate sodium salt) with various block lengths and block ratios were synthesized by reversible addition-fragmentation chain transfer (RAFT) [33] technique, and molecular properties and self-assembling behavior were duly investigated. Especially, temperature responsivity and effect of salt addition to these properties and assembling behavior were systematically studied. Since the block copolymer should be ionic amphiphilic block copolymer above LCST, non-surface active behavior is expected; switching between non-surface active and surface active character is expected in addition to unimer/micelle transition. In this study, we challenged to control non-surface active/surface active transition by changing solution temperature and added salt concentration.

Experimental

Materials

N-isopropylacrylamide (NIPAm) (G.R.), styrenesulfonate sodium salt (SSNa), and azobisisobutylonitrile (AIBN) (G.R.) were purchased from Wako Pure Chemical (Osaka, Japan). NIPAm was dissolved into *n*-hexane at 40 °C and recrystallized in a refrigerator. After removing the supernatant, NIPAm crystals were washed in *n*-hexane and dried in vacuo. The chain transfer agent for RAFT polymerization was α-methyl trithiocarbonate-S-phenylacetic acid (TCTA), which was synthesized by the method reported previously [34]. *N*,*N*-dimethylformamide (DMF) and *n*-hexane were purchased from Wako and used as received. *N*-methylformamide (NMF) was a product of Nacalai tesque (Kyoto, Japan). The water used was ultrapure water obtained by a Milli-Q system (18.2 MΩ).

Synthesis of block copolymer

PNIPAm-*b*-PSSNa was synthesized by RAFT polymerization as shown in Scheme 1. The typical procedure is as follows. First, the PNIPAm homopolymer was synthesized. NIPAm, AIBN, and TCTA were mixed into a Schlenk tube at a molar ratio of 100:0.25:1. Then, the solvent, DMF, was added. The solution was degassed by freeze-pump-thaw cycles three times. Polymerization reaction was carried out at 70 °C under an Ar atmosphere for 4 or 6 h. The reaction was stopped by ice-cooling. The polymer thus obtained was purified by dialysis against pure water for 1 week, and then lyophilized. The block copolymers were synthesized by the RAFT method in a manner similar to the PNIPAm homopolymer thus synthesized as a macro-CTA. The sample mixture was degassed three times by a freeze-pump-thaw cycle. The mixing ratio, i.e., PNIPAm:SSNa:AIBN, was 1:100:1 or 1:150:1, and the reaction was carried out in NMF solvent at 80 °C. The reaction time was 4 or 6 h. The block copolymer thus obtained was purified by dialysis against ultrapure water and lyophilized.

Gel permeation chromatography

The molecular weight and its distribution were evaluated by a JASCO gel permeation chromatography (GPC) system composed of an RI-965 RI detector, UV2075 Plus UV detector, PU-980 pump, DG-980-50 degasser, and CO-965 column oven. The column used was Shodex KF804L with THF as an eluent and polystyrene standards.

^{1}H nuclear magnetic resonance

^{1}H nuclear magnetic resonance (NMR) spectra were obtained with a JEOL JNM AL-400 and JNM EX-400 spectrometer.

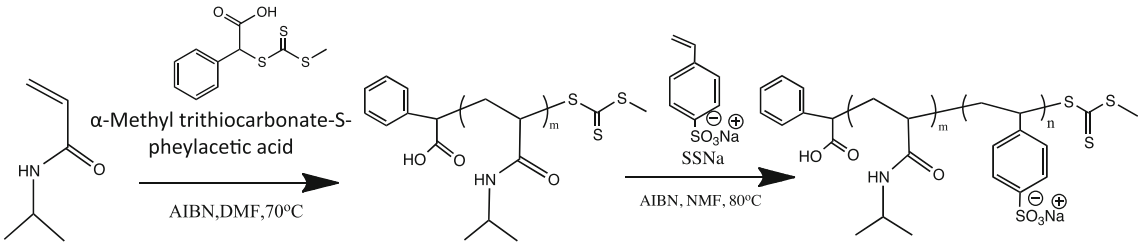

Scheme 1 Synthesis of PNIPAm-*b*-PSSNa

The polymer concentration was 1 wt%, and the solvents were $CDCl_3$ (EURISO-TOP 99.8%) and D_2O (99.9%, Cambridge Isotope Laboratory, U.K.).

Turbidity

Cloud point and CMT for 1 mg/ml polymer solutions were determined by turbidimetry with a U-3310 UV/VIS spectrometer (Hitachi, Tokyo, Japan). Cloud point was determined by the temperature at which the turbidity at 500 nm started to increase. CMT was defined by the temperature at which the turbidity became 50% of the saturated turbidity value. The temperature of the solution was controlled with a water-jacketed cell holder equipped with a Thermo Neslab RTE-7 water-circulating bath.

Static light scattering

Static light scattering (SLS) intensity was measured as a function of polymer concentration at 25 and 50 °C to determine the cmc. Sample solutions with various concentrations were prepared by repeating dilution. SLS instrument used was Photal SLS-7000 system (Otsuka Electronic, Osaka, Japan) with a 15 mW He-Ne laser of 632.8 nm wavelength (λ). The scattering angle (2θ) was 90°.

Surface tension

Surface tension of the solutions was measured by the Wilhelmy method with a FACE CBVP-Z surface tensiometer (Kyowa Interface Science Co., Ltd. (Tokyo, Japan)), using a Pt plate in full automatic mode. Measurements were carried out 24 h after the solution was put into the glass cell without disturbance.

Foam formation observation

Foam formation behavior was observed after 1 min shaking followed by 1 min standing without disturbance. For observation at 50 °C, the sample bottle was immersed in 50 °C water before shaking for 10 min.

X-ray reflectivity

X-ray reflectivity (XR) measurements were performed for 1-mg/ml aqueous solution of $(NIPAm)_{74}$-*b*-$(SSNa)_{50}$ at 25 and 50 °C. The details of XR instruments and data analysis were fully described previously [35–39]. To avoid solvent (water) evaporation, we covered the sample container with a plastic (acryl resin) box which had a Kapton window for the X-ray path.

Dynamic light scattering

Dynamic light scattering (DLS) measurements were carried out at 50 °C to estimate the hydrodynamic radius (R_h) with a Photal SLS-7000 system connected with a GC-1000 correlator (Otsuka Electronic, Osaka, Japan). The time correlation function was measured at scattering angles of 60°, 75°, 90°, and 105°, and it was analyzed by a single exponential fitting. The accumulation time was 30 min. After the linearity of the decay rate Γ as a function of q^2 (q: scattering vector, $q = 4\pi n \sin\theta/\lambda$, n: the refractive index of the solvent) was confirmed, the translational diffusion coefficient D was evaluated from the slope of this straight line. R_h was calculated by the Stokes-Einstein relation, i.e., $R_h = kT/6\pi\eta D$, where k is the Boltzmann constant, T the absolute temperature, and η the viscosity of the solvent. The details of DLS data analysis were fully described elsewhere [40].

Transmission electron microscopy

Transmission electron microscopy (TEM) micrographs were taken at the Hyogo Prefecture University with JEOL JEM-2100 at 200 kV. $(NIPAm)_{74}$-*b*-$(SSNa)_{50}$ aqueous solution was allowed to stand in a 50 °C water bath for 10 min. The surface of the Cu TEM grid (200 mesh with coating) was hydrophilically modified by plasma irradiation. The TEM grid was put and kept on the 50 °C hotplate for 10 min, and a sample solution of 50 °C was dropped on the grid. After wiping off the excess solution, 0.2% sodium phosphotungstate 50 °C solution was dropped on the grid. Excess solution was removed by wiping and then dried in vacuum for 1 day.

Results and discussion

Characteristics of block copolymers synthesized.

Tables 1 and 2 show the characteristics of homo and block copolymers thus synthesized evaluated by GPC and NMR. The degree of polymerization (m) and the distribution of PNIPAm homopolymers were evaluated by GPC, and block ratio, m:n, was estimated by NMR spectra shown in Fig. 1. n values were calculated from m value by the peak area ratio of ^{1}H NMR spectra shown in Fig. 1. The sample (a) m:n = 72:340 could be used only for limited experiments since its amount was so small (yield: 24% for sample (a), about 60% for other polymers).

Determination of cloud point of PNIPAm and block copolymers

The cloud point of PNIPAm homopolymer was determined by turbidity measurements (Fig. S1 in Supporting Information (SI)). The same cloud point was found for $(NIPAm)_{40}$ and $(NIPAm)_{74}$, and it was observed to decrease with increasing salt (NaCl) concentration, as was reported by Cremer et al. [41] and as we found previously [39, 42]. FigURE 2 shows the temperature dependence of turbidity of block copolymer aqueous solutions at different salt concentrations. Only typical examples are shown in Fig. 2, and whole dataset for all the polymers (a)-(f) are shown in Fig. S2 in Supporting Information to save space. At low temperature, turbidity was 0%, i.e., it was clear solution. With elevating temperature, turbidity stared to increase at certain temperature, then it was saturated at certain value. This means that polymers associated/aggregated in solution at certain temperature. The cloud point was indicated by arrow in the figure, and it decreased with increasing salt concentration. It is interesting to note that the turbidity above cloud point is not so high (50% or low) and decreased with increasing salt concentration. In other words, the solution becomes more transparent above cloud point with increasing salt concentration. This suggests the self-assembly formation of block copolymer. PNIPAm homopolymer makes a large aggregate in a solution above LCST, which results in high turbidity of the solution. However, block copolymer can form self-assembly such as a micelle; the turbidity of the solution is not so high [31]. As will be shown in Fig. 10, the solutions under this condition looked bluish, which is reminiscent of a micelle formation. Hence, the cloud point here can be called CMT. This point, i.e., self-assembly formation, will be examined by DLS measurement later. CMT thus estimated was plotted as a function of salt concentration in Fig. 3. The CMT decreased with added salt concentration. This trend is similar to that for PNIPAm homopolymer, and this might be a result of acceleration of dehydration by salt ions [41]. The effect of chain length is not so clear but it looks that the CMT of the block copolymer having a relatively large portion of hydrophilic chain is higher (e.g., samples (c) and (e)). This might be due to higher solubility of polymer chain.

Table 1 Characteristics of PNIPAm homopolymer

PNIPAm	DP[a]	Mw/Mn[a]
P1	40	1.26
P2	74	1.28
P3	80	1.21

[a] Determined by GPC with THF as an eluent

Effects of temperature and salt concentration on cmc

Static light scattering experiments as a function of polymer concentration were performed at 25 and 50 °C to determine the cmc. Figures 4 and S3 show the results for six block copolymers. At 25 °C where PNIPAm is water soluble, the SLS intensity was very weak for all six block copolymers. This indicated that block copolymers were molecularly dissolved in water since both PNIPAm and PSSNa blocks are water-soluble (not perfectly straight line at 25 °C may be some sign of aggregation of PNIPAm chain even at room temperature. But this is out of scope of this study). One may notice that SLS intensity for $NIPAm_{40}$-b-$SSNa_{28}$ is slightly stronger than the other five, but this may be due to the very short SSNa block (n = 28), which lowers the solubility of block copolymer and they probably form a slightly larger aggregate in solution. On the other hand, a clear bending point was found at 50 °C for all six block copolymers, which should correspond to cmc. This is quite natural because PNIPAm is not water soluble at this temperature, so all of these block copolymers are amphiphilic under this condition. The cmc values thus evaluated at 50 °C were plotted as a function of salt (NaCl) concentration in Fig. 5. Although not perfect, the tendency that the polymer with a longer PSSNa block compared to PNIPAm block has higher cmc value. What is interesting is its salt concentration dependence: cmc increased with increasing salt concentration. This opposes to the famous Corrin-Harkins law for ionic surfactants [20]. A similar tendency was observed for all "non-

Table 2 Characteristics of block copolymers

PNIPAm-*b*-PSSNa	m:n[a]
a	72:340
b	40:28
c	40:78
d	74:50
e	74:115
f	80:73

[a] Determined by ^{1}H NMR

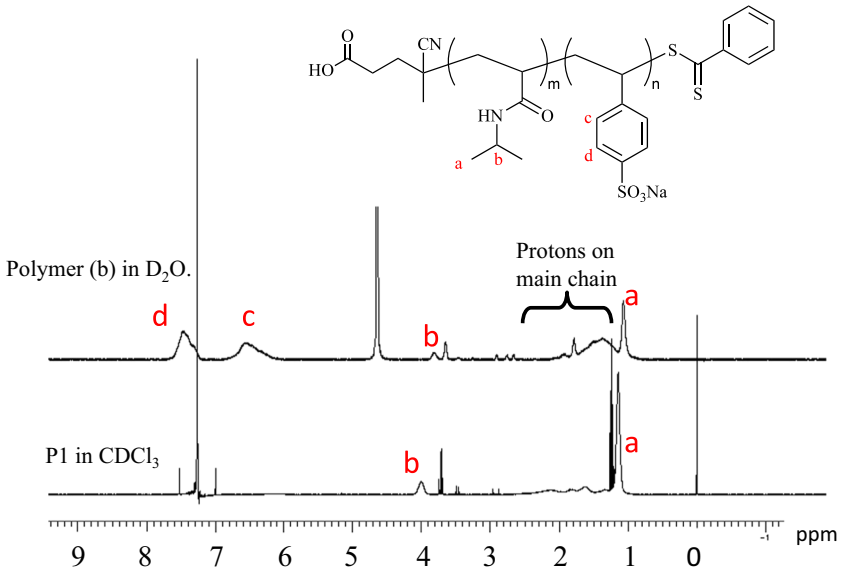

Fig. 1 ^{1}H NMR spectra for PNIPAm homopolmer (P1) in $CDCl_3$ and PNIPAm-*b*-PSSNa block copolymer (**b**) in D_2O

surface active" polymers ever studied by us [19]. This observation may mean that PNIPAm-*b*-PSSNa block copolymers have a non-surface active nature to some extent under this condition. This negative Corrin-Harkins behavior can be explained as follows [19]. With increasing salt concentration, the image charge repulsion is shielded by added salt ions. Then, the polymers can be adsorbed at the air/water interface, which results in hard to form micelles in bulk. So, micelles can be formed at higher concentration, i.e., cmc increases.

Effects of temperature and salt concentration on adsorption behavior at the air/water interface

Surface tension of the solutions of six block copolymers was measured as a function of polymer concentration at different added salt concentrations both at room temperature and at 50 °C. In Fig. 6, the difference of surface tension between polymer solution and pure solvent, Δsurface tension, was plotted with polymer concentration. This is because the surface tension of solvent (water) depends on temperature and added salt concentration. The surface tension decreased with increasing polymer concentration, jn which behavior is quite normal for a surface active agent. However, this result was quite unexpected since non-surface active nature was observed for cmc as a function of added salt concentration (Fig. 5). Judging from this surface tension dataset, these polymers are surface active. In surface tension-polymer concentration curves in Fig. 6, the bending point was observed, although not clear, which should correspond to cmc. However, this bending point was located around 0.01–0.1 mg/ml in while cmc values by SLS were about 0.001–0.01 mg/ml, one order of magnitude lower. At the cmc by SLS, the surface tension is in the way to decrease. This tendency is also observed for "weakly non-surface active" polymers [19]. Non-surface active polymers do not show decrease of surface tension of the solution, but slight decreased with polymer concentration after addition of a small amount of salt. The surface active nature was suppressed and finally disappeared after addition of a large

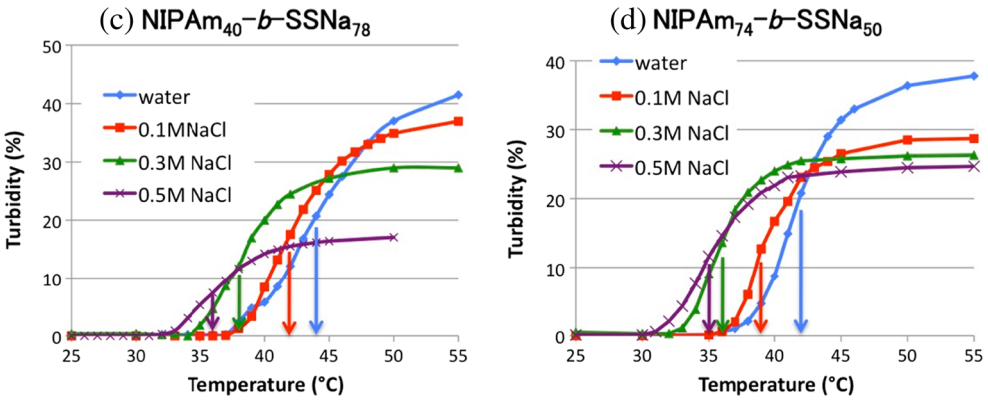

Fig. 2 Temperature dependence of turbidity for 1-mg/ml PNIPAm-*b*-PSSNa aqueous solutions. Sample: **c** $NIPAm_{40}$-*b*-$SSNa_{78}$, **d** $NIPAm_{74}$-*b*-$SSNa_{50}$. Arrows indicate the critical micelle temperature (CMT). Dataset for all the polymers **a**–**f** are shown in Fig. S2 in Supporting Information

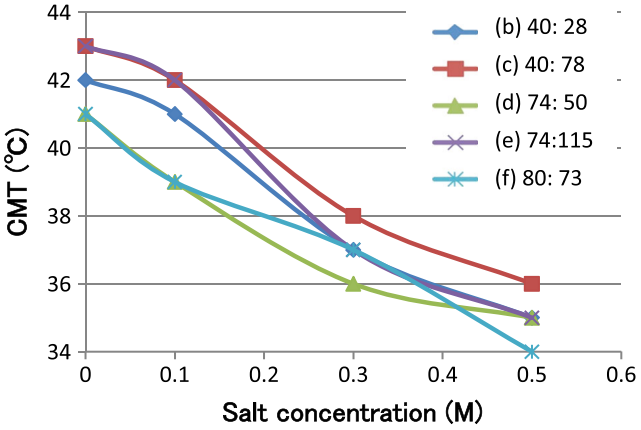

Fig. 3 Salt concentration dependence of CMT in water for samples (**b**–**f**). [polymer] = 1 mg/ml. This polymer weight concentration corresponds to 9.51×10^{-5}, 4.80×10^{-5}, 5.30×10^{-5}, 3.10×10^{-5}, and 4.12×10^{-5}, for **b**–**f**, respectively, in (polymer mole)/liter

amount of salt. Hence, this "disagreement" between cmc by SLS and "apparent" cmc by surface tension means that these polymers are weakly non-surface active although surface tension decreases to some extent.

Salt concentration dependence was not clearly observed in Fig. 6. For (c) $NIPAm_{40}$-*b*-$SSNa_{78}$ and (e) $NIPAm_{74}$-*b*-$SSNa_{115}$, relatively longer SSNa chain polymers, the surface tension decreased with increasing salt concentration. However, for (b) $NIPAm_{40}$-*b*-$SSNa_{28}$, (d) $NIPAm_{74}$-*b*-$SSNa_{50}$, and (f) $NIPAm_{80}$-*b*-$SSNa_{73}$ which have relatively shorter SSNa chains, did not have clear dependency and it was not in the order of salt concentration. We cannot explain this observation yet.

For temperature dependence, quite interesting behavior was observed. For relatively longer SSNa polymers including (a) $NIPAm_{72}$-*b*-$SSNa_{340}$, the surface tension at 50 °C was higher than that at room temperature while no large difference was found for polymers with shorter SSNa chains, i.e., (b), (d), and (f). This observation might be related to the non-surface active nature. At 50 °C, the PNIPAm chain became hydrophobic, and the block polymers formed micelles. The block copolymer became amphiphilic and so the surface tension of the solution should be lower than that at room temperature, in which behavior is normal for a surfactant. However, in this case, the block copolymer becomes amphiphilic but not so surface active, i.e., it might be slightly non-surface active polymers. As clarified by our systematic continuous study, the origin of the non-surface activity is the strong image charge repulsion between the water surface and ionic polymer block and a very stable micelle formation in the bulk due to macromolecular nature of hydrophobic chain and hydrophilic ionic corona chains [2–7, 19]. For longer SSNa chain polymers, the image charge repulsion is stronger, so adsorption of the block copolymer at the water surface was suppressed. As a result, the surface tension of the solution was larger than that at room temperature, where block copolymers are totally hydrophilic and molecularly dissolved (i.e., no micelle). It may be noteworthy that the homopolymer of both PNIPAm and PSSNa is surface active.

As discussed above, some characteristics for "weakly" non-surface active polymers were observed, but it is certain that the surface tension itself is decreased clearly, which could be discrepancy. Hence, to obtain more detailed information for the situation of solution surface, we performed X-ray reflectivity (XR) experiments for solutions of $NIPAm_{74}$-*b*-$SSNa_{50}$ at 25 and 50 °C with and without 0.5 M NaCl. XR profiles with fitting curve and the density profile normal to the water surface thus evaluated are shown in Fig. 7, and the fitting parameters, i.e., thickness and density of each layer and interface roughness, are tabulated in Table 3. At 25 °C, since the block copolymer is water soluble, PNIAPAm, which is surface active, adsorbed at the water surface and PSSNa forms brush layer under the PNIPAM layer [35–38]. After addition of 0.5 M NaCl, PNIPAm layer became thinner but had higher density probably due to dehydration. At 50 °C, the PNIPAm layer, which is now hydrophobic, formed on the water surface. A carpet layer of PSSNa, which is a dense PSSNa layer, was formed just beneath the water surface to avoid direct contact between the hydrophobic PNIPAm layer and water, as was observed for all ionic amphiphilic diblock copolymer

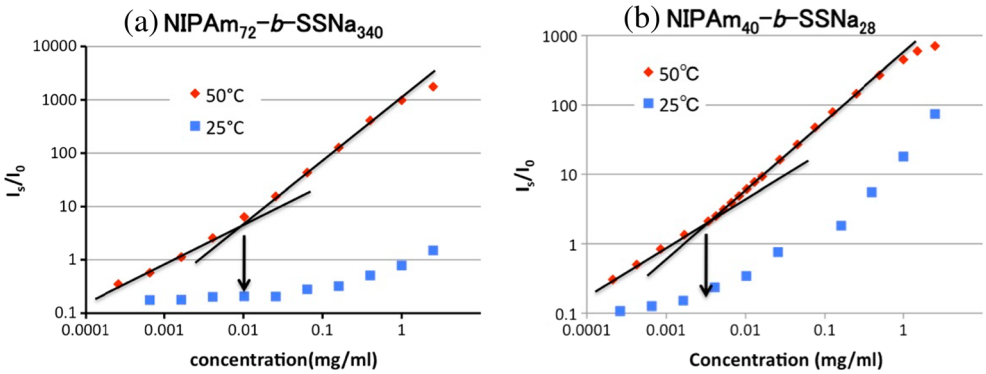

Fig. 4 SLS intensity for PNIPAm-*b*-PSSNa water solutions at 25 and 50 °C. Arrows indicate cmc at 50 °C. Dataset for all the polymer (**a**–**f**) is shown in Fig. S3 in Supporting Information

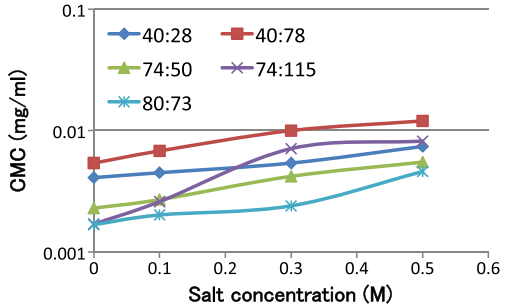

Fig. 5 Salt concentration dependence of CMC

monolayer ever studied [35–38]. Under the carpet layer, a PSSNa brush layer was found and the brush chain shrunk as was again the case for other polymers ever studied. Nanostructures of the adsorbed monolayer observed here are schematically shown in Fig. 8. By XR technique, polymer adsorption has been directly confirmed in molecular scale. Hence, now, the apparent discrepancy between this observation and cmc behavior with salt should be our further subject.

As is well known, foam is an increase of surface area by the increase of interfacial energy obtained from kinetic energy, and foam is stabilized by adsorption of a surface active agent at the air/water interface [43]. Hence, since foam formation is strongly related to adsorption behavior, foam formation behavior was duly investigated. Figure 9 shows foam formation behavior for $NIPAm_{72}$-*b*-$SSNa_{340}$ (sample (a)) at room temperature and at 50 °C. At room temperature, foam formation

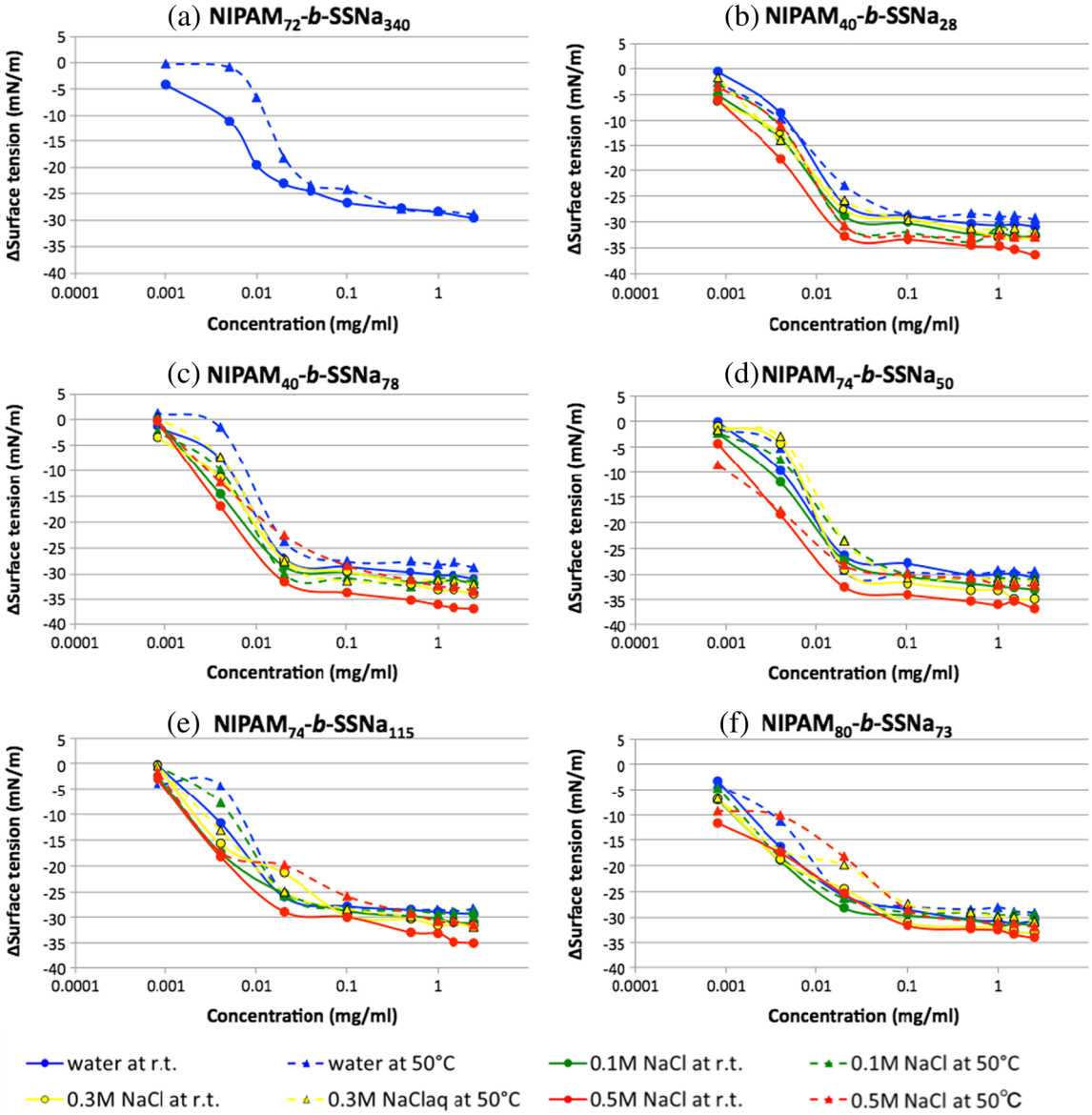

Fig. 6 Concentration dependence of Δsurface tension with different added salt concentrations at room temperature and at 50 °C. ΔSurface tension is the difference of surface tension of solution from pure solvent

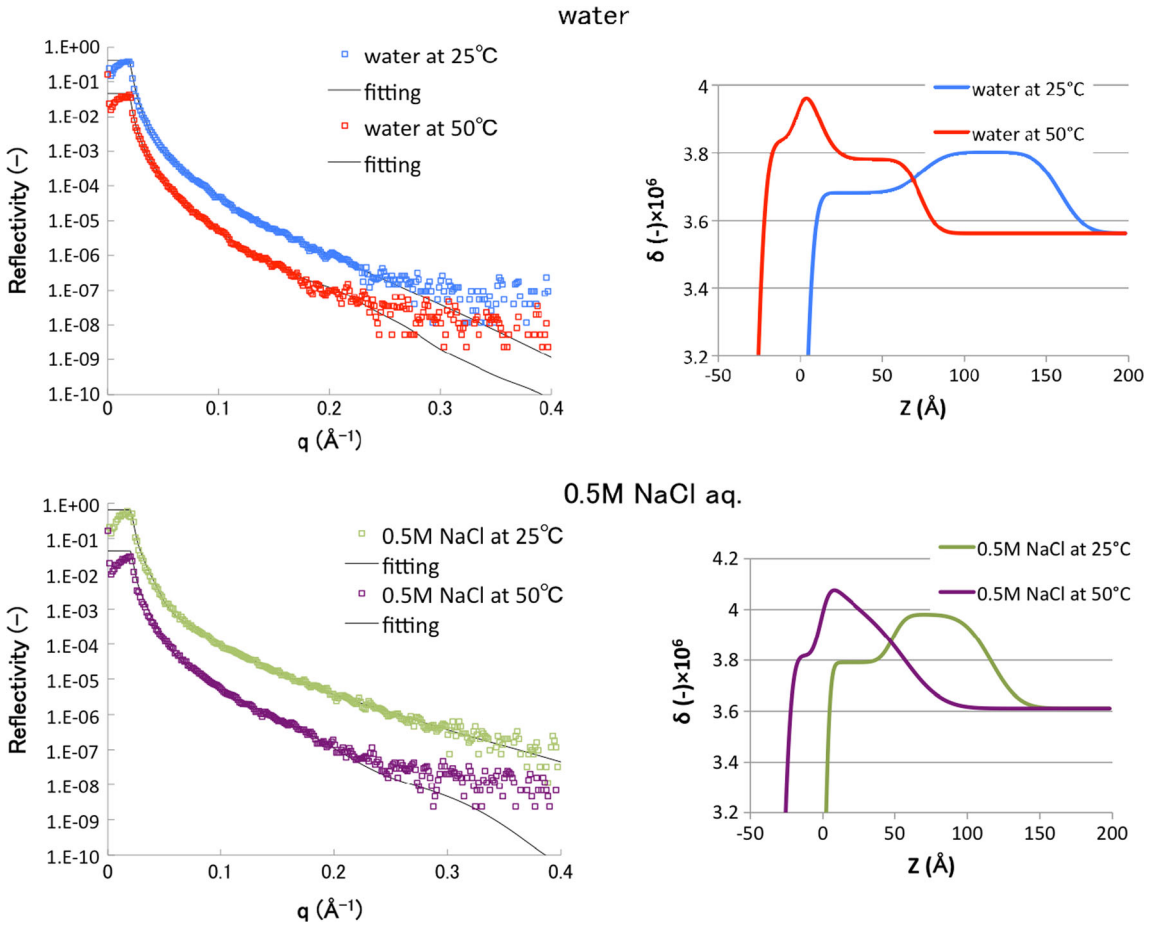

Fig. 7 XR profiles (left) and density profiles (right) of **d** NIPAm$_{74}$-*b*-SSNa$_{50}$ adsorbed monolayer at the water surface (top) and 0.5 M NaCl aq. (bottom)

was observed but no foam was found at 50 °C. Foam formation behavior for other polymers with different salt concentrations is shown in Figs. 10 and S4. At room temperature in which polymers are molecularly dissolved in water, all the polymer solutions showed foam formation, which means that polymers are surface active and slightly good foam formation

Table 3 Fitting parameter of (d) NIPAm$_7$4-*b*-SSNa$_5$0 adsorbed monolayer at the water surface and 0.5 M NaCl aq. by XR

solution	PNIPAm Layer			PSSNa carpet layer			PSSNa brush layer			subphase
	$\delta_1 \times 10^6$	d_1 (Å)	σ_1	$\delta_2 \times 10^6$	d_2 (Å)	σ_2	$\delta_3 \times 10^6$	d_3 (Å)	σ_3	σ
water at 25°C	3.68	75	5.8				3.8	85	12	12
water at 50°C	3.84	30	6.3	4.1	10	5	3.78	65	10	8
0.5M NaCl at 25°C	3.79	50	3.7				3.98	68	7	15
0.5M NaCl at 50°C	3.85	30	6	4.2	9	5	3.98	50	20	20

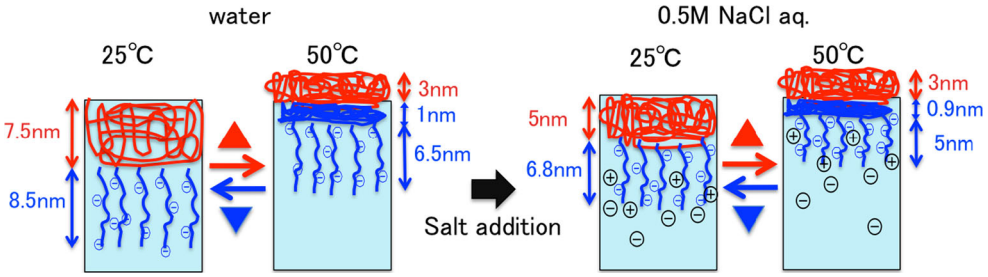

Fig. 8 Schematic representation of temperature and salt concentration dependence of the nanostructure of **d** $NIPAm_{74}$-*b*-$SSNa_{50}$ adsorbed monolayer

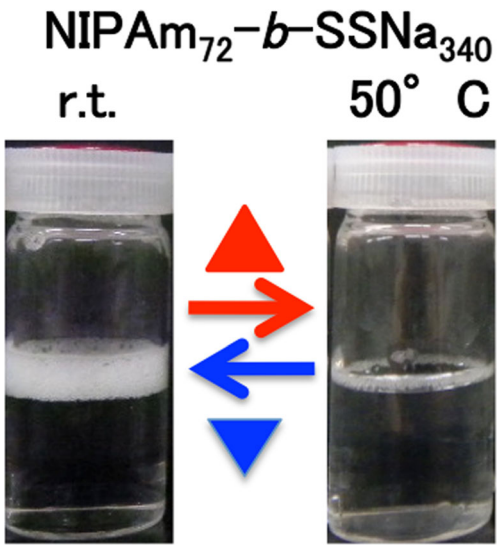

Fig. 9 Observation of foam formation for 1 mg/ml (**a**) $NIPAm_{72}$-*b*-$SSNa_{340}$ aqueous solution

could be noticed at higher salt concentration. At 50 °C, none of the polymers showed foam formation without added salt. This means that the polymers under this condition had a non-surface active nature; micelle formed in bulk solution but little polymers were adsorbed at the air/water interface due to an image charge repulsion and stable micelle formation. Including higher concentrations of added salt, the solution itself looks bluish, which means micelle formation in bulk. By addition of salt, good foam formation was observed, which means that the polymers have surface active nature due to shielding effect of image charge repulsion by salt ions, which is in good agreement with other non-surface active polymers studied so far.

Evaluation of the size of micelle by DLS

The hydrodynamic radius, R_h of micelles, was evaluated by DLS. The typical time correlation function of scattered field, $g^{(1)}(q,\tau)$, is shown in Fig. S5(A), and an example of Γ vs. q^2

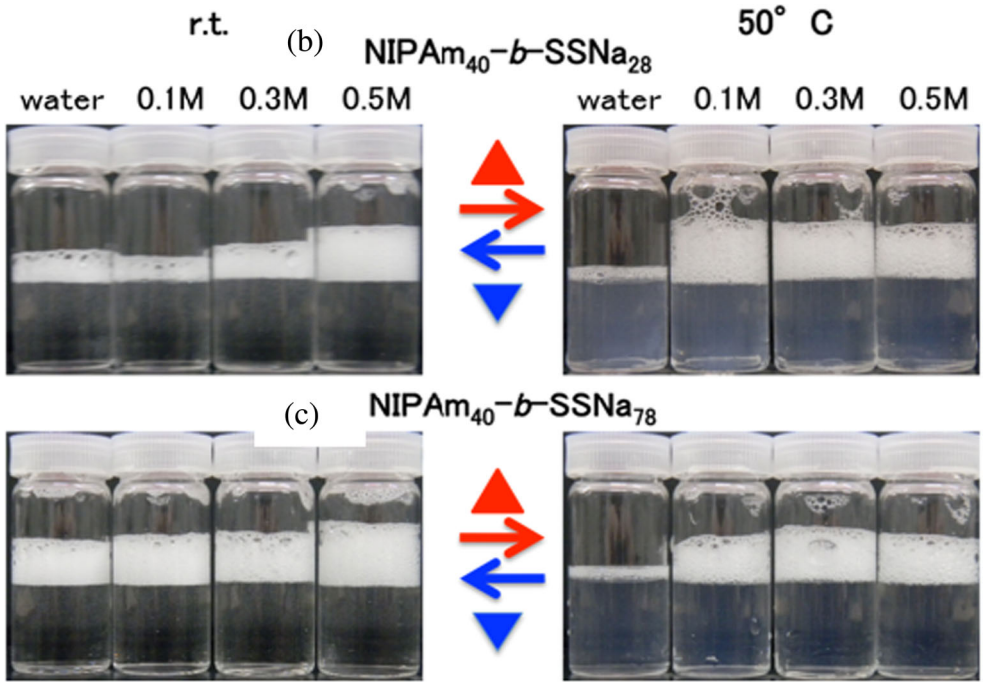

Fig. 10 Observation of foam formation for 1 mg/ml PNIPAm-*b*-PSSNa aqueous solutions. Dataset for all the polymer (**b**–**f**) is shown in Fig. S4 in Supporting Information

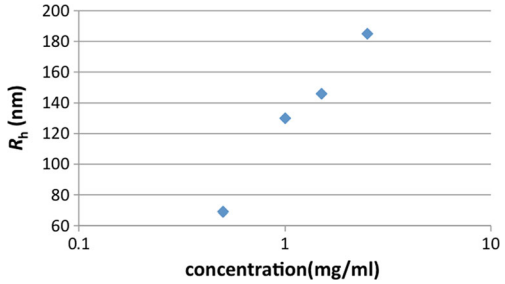

Fig. 11 Polymer concentration dependence of R_h for **a** $NIPAm_{72}$-*b*-$SSNa_{340}$ aqueous solution at 50 °C

plot is shown in Fig. S5(B) in SI. A polymer concentration dependence of R_h for polymer (a), $NIPAm_{72}$-*b*-$SSNa_{340}$, is shown in Fig. 11. R_h value increased with increasing polymer concentration. This is an unexpected result: the size of the polymer micelle was mostly unaffected by the polymer concentration [4], since the size and shape of the micelle are generally determined by the critical packing parameter proposed by Israelachivili [44]. In fact, the size of the micelles we studied previously did not show polymer concentration dependence [3], and this is our first experience. R_h at 2.5 mg/ml was 185 nm, which is not so large compared to the fully stretched chain length (f.s.c.l.), 103 nm, for vinyl polymer of total degree of polymerization of 412 (= 72 + 340). In most of our previous studies, R_h of polymer micelle was larger than f.s.c.l. by a factor of 1.2–2.0. This is due to the fact that polymer micelle is not hard sphere but with hairy corona on its surface. R_h was calculated by the Stokes-Einstein equation, which is for a hard sphere. However, the real polymer micelle has hairy corona, so large friction with solvent should occur, which results in slow diffusion, and hence results in apparently larger R_h. In this case, the factor was less than 2.0, so it is not unnatural to think that spherical polymer micelle is formed in this solution. This is also justified by the concept of the critical packing parameter [44]; this polymer (a) has large head group, so it prefers a spherical

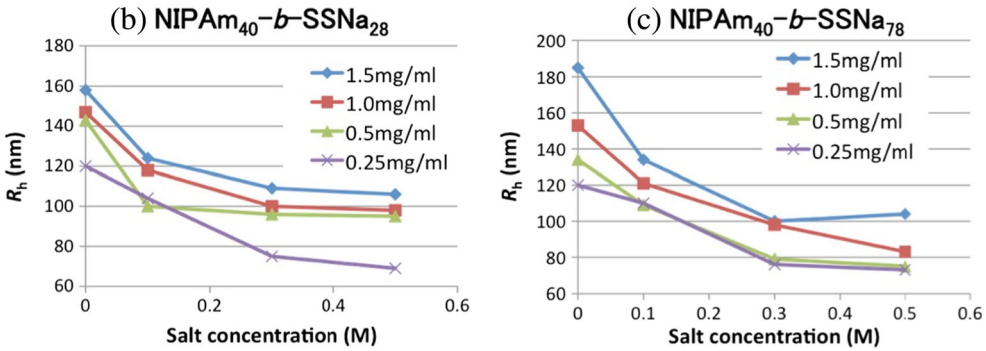

Fig. 12 Salt concentration dependence of R_h of PNIPAm-*b*-PSSNa micelles at 50 °C. Dataset for all the polymer (**b**–**f**) is shown in Fig. S6 in Supporting Information

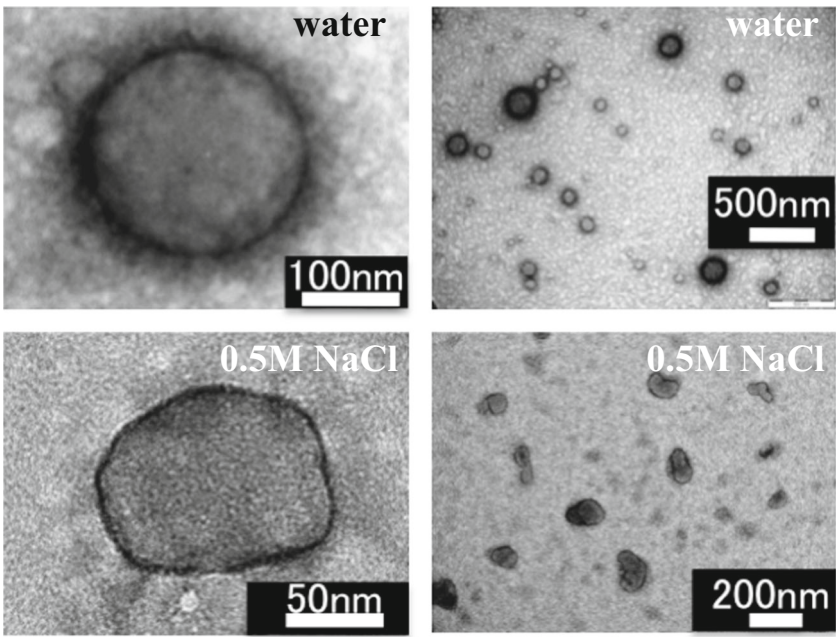

Fig. 13 TEM images for 1.5 mg/ml (**d**) $NIPAm_{74}$-*b*-$SSNa_{50}$ in water (above) and in 0.5 M NaCl aq. (below)

micelle. However, the strange increase of R_h may mean larger particle formation, such as vesicle, as will be discussed later.

Figures 12 and S6 show R_h values for other polymers at different polymer concentration with various added salt concentrations. As was for polymer (a) in Fig. 11, R_h increased with increasing polymer concentration for all the polymers. For all polymers here, the evaluated R_h values are fairly large compared to f.s.c.l. of each polymer. Hence, it is difficult to assume spherical micelle formation. Also, for all polymers, R_h decreased with increasing added salt concentration. In our previous studies, R_h also decreased with added salt concentration, and this was interpreted by shrinking of ionic corona chains by an electrostatic shielding effect of added salt ions. In the present cases, the same phenomenon should occur by salt addition, but what we should notice is its amount of decrease; for example, the decrease of R_h for polymer (d) 74:50 sample was almost 100 nm by 0.5 M NaCl addition. This is too large since this length is larger than the f.s.c.l. of $SSNa_{50}$ (32 nm). Hence, the possibility of another structure change should be taken into account. Then, we performed TEM observation. Figure 13 is TEM images of polymer (d) $NIPAm_{74}$-*b*-$SSNa_{80}$ in pure water (above) and in 0.5 M NaCl (below) at 50 °C. In water, a large spherical particle with radius of about 130 nm was clearly seen with higher contrast at the particle surface, which is reminiscent of vesicle formation. This size is in good agreement with R_h value, although slightly smaller, since the corona chains should shrink up in drying process in TEM sample preparation. Vesicle formation for polymer (d) is naturally understandable by the concept of the critical packing parameter since it has almost the same block length of the hydrophobic and hydrophilic segments. A similar vesicle-like particle with radius of about 60 nm is clearly observed for 0.5 M NaCl condition. A large decrease in size by salt addition was also confirmed by TEM observation. Sharp and angular particle surface for 0.5 M NaCl may be due to corona shrinking and/or dehydration of PNIPAm chains although its details are not clear at this stage. Further confirmation by other techniques, e.g., Cryo-TEM etc., is our future target.

Conclusions

PNIPAm-*b*-PSSNa block copolymers with various block length and length ratios were synthesized by RAFT polymerization. The molecular properties such as surface activity, adsorption behavior at the water surface, and micelle formation behavior were duly investigated as a function of polymer concentration, added salt concentration, and solution temperature. At room temperature where PNIPAm block is water soluble, the block copolymers molecularly dissolved in water. However, at a temperature higher than LCST, where the PNIPAm block becomes hydrophobic, these block copolymers behave as an ionic amphiphilic diblock copolymer and showed some typical behaviors for non-surface active polymers. However, the surface tension of the solution itself clearly decreased with polymer concentration, which is, needless to say, a behavior for surface active agent. Hence, we should mention that PNIPAm-*b*-PSSNa block copolymers have both characteristics for non-surface active polymers and also for surface active agent, although its origin is unclear at this moment. Something special might exist for PNIPAm containing block copolymers and/or novel concept might be required for the correlation between polymer adsorption and surface activity. In solutions, micelles or large vesicle-like particles were formed, and their size was increased with polymer concentration and became smaller by salt addition. Studies of block copolymers of PNIAPm with different ionic polymers are our future target.

Acknowledgements This work was supported by a grant-in-aid for Scientific Research on Innovative Areas “Molecular Soft-Interface Science” (20106006) from the Ministry of Education, Culture, Sports, Science and Technology of Japan, to which our sincere gratitude is due. Our great appreciation goes to Dr. Arjun Ghosh, Dr. Murugaboopathy Sivanantham, and Dr. Saurabh Shrivastava for their fruitful suggestions and discussions as a post-doctoral fellow in our research group.

Compliance with ethical standards

Conflict of interest The authors declare that they have no conflict of interest.

References

1. Hamley I (2005) Block copolymers in solution, fundamentals and applications. Wiley, Chapter 4
2. Matsuoka H, Chen H, Matsumoto K (2012) Molecular weight dependence of non-surface activity for ionic amphiphilic Diblock copolymers. Soft Matter 8(35):9140–9146
3. Shrivastava S, Matsuoka H (2014) Photo-responsive block copolymer: synthesis, characterization and surface activity control. Langmuir 30(14):3957–3966
4. Ghosh A, Yusa S, Matsuoka H, Saruwatari Y (2014) Chain length dependence of non-surface activity and micellization behavior of cationic amphiphilic diblock copolymers. Langmuir 30(12):3319–3328
5. Murugaboopathy S, Matsuoka H (2015) Salt-dependent surface activity and micellization behaviour of zwitterionic amphiphilic diblock copolymers having carboxybetaine. Coll Polym Sci 293(5):1317–1328
6. Matsuoka H, Onishi T, Ghosh A (2014) pH responsive non-surface active / surface active transition of weakly ionic amphiphilic diblock copolymers. Coll Polym Sci 292(4):797–806
7. Matsuoka H, Matsutani M, Mouri E, Matsumoto K (2003) Polymer micelle formation without Gibbs monolayer formation—synthesis and characteristics of amphiphilic diblock copolymer having sulfonic acid groups. Macromolecules 36(14):5321–5330
8. Matsuoka H, Maeda S, Kaewsaiha P, Matsumoto K (2004) Micellization of non-surface-active diblock copolymers in water. Special characteristics of poly(styrene)-block-poly(styrenesulfonate). Langmuir 20(18):7412–7421

9. Onsager L, Samaras NNT (1934) The surface tension of Debye-Hückel electrolytes. J Chem Phys 2:528
10. Amiel C, Sikka M, Schneider JW, Tsao YH, Tirrell M, Mays JW (1995) Adsorption of hydrophilic-hydrophobic block copolymers on silica from aqueous solutions. Macromolecules 28(9):3125–3134
11. Jacquin M, Muller P, Cottet H, Théodoly O (2010) Self-assembly of charged amphiphilic diblock copolymers with insoluble blocks of decreasing hydrophobicity: from kinetically frozen colloids to macrosurfactants. Langmuir 26(24):18681–18693
12. Théodoly O, Jacquin M, Muller P, Chhun S (2009) Adsorption kinetics of amphiphilic diblock copolymers: from kinetically frozen colloids to macrosurfactants. Langmuir 25(2):781–793
13. Wittmer J, Joanny JF (1993) Charged diblock copolymers at interfaces. Macromolecules 26(11):2691–2697
14. An SW, Su TJ, Thomas RK, Baines FL, Billingham NC, Armes SP, Penfold J (1998) Neutron reflectivity of an adsorbed water-soluble block copolymer: a surface transition tomicelle-like aggregates at the air/water interface. J Phys Chem B 102(2):387–393
15. An SW, Su TJ, Thomas RK, Baines FL, Billingham NC, Armes SP, Penfold J (1998) Neutron reflectivity of adsorbedwater-soluble block copolymers at the air/water interface: the effects of composition and molecular weight. Macromolecules 31(22):7877–7885
16. Iddon PD, Robinson KL, Armes SP (2004) Polymerization of sodium 4-Styrenesulfonate via atom transfer radical polymerization in Protic media. Polymer 45(3):759–768
17. Eghbali E, Colombani O, Drechsler M, Muller AHE, Hoffmann H (2006) Rheology and phase behavior of poly(n-butyl acrylate)-blockpoly(acrylic acid) in aqueous solution. Langmuir 22(10):4766–4776
18. Garnier S, Laschewsky A (2006) New amphiphilic diblock copolymers: surfactant properties and solubilization in their micelles. Langmuir 22(9):4044–4053
19. Kaewsaiha P, Kozo M, Matsuoka H (2005) Non-surface activity and micellization of ionic amphiphilic diblock copolymers in water. Hydrophobic chain length dependence and salt effect on surface activity and the critical micelle concentration. Langmuir 21(22):9938–9945
20. Corrin ML, Harkins WD (1947) The effect of salts on the critical concentration for the formation of micelles in colloidal electrolytes. J Am Chem Soc 69(3):683–688
21. Minko S (2006) Responsive polymer materials: design and applications. Blackwell Publishing, Ames,
22. Schild HG (1992) Poly(N-Isopropylacrylamide): experiment, theory and application. Prog Polym Sci 17:163–249
23. Scapra JS, Mueller DD, Klotz IM (1967) Slow hydrogen-deuterium exchange in a non-a-helical polyamide. J Amer Chem Soc 89(24):6024–6030
24. Heskins M, Guillet JE (1968) Solution properties of poly(*N*-isospropylacrylamide). J Macromol Sci-Chem A2(8):1441–1455
25. Winnik FM (1990) Fluorescence studies of aqueous solutions of poly(*N*-isopropylacrylamide) below and above their LCST. Macromolecules 23(1):233–242
26. Cölfen H (2001) Double-hydrophilic block copolymers: synthesis and application as novel surfactants and crystal growth modifiers. Macromol Rapid Commun 22(4):219–252
27. Bütün V, Billingham NC, Armes SP (1998) Unusual aggregation behavior of a novel tertiary amine methacrylate-based diblock copolymer: formation of micelles and reverse micelles in aqueous solution. J Am Chem Soc 120(45):11818–11819
28. Vishnevetskaya NS, Hildebrand V, Niebuur BJ, Grillo I, Filippov SK, Laschewsky A, Müller-Bushbaum P, Papadakis CM (2016) Aggregation behavior of doubly Termorenponsive Polysulfobetaine-*b*-poly(*N*-isopropylacrylamide) Diblock copolymers. Macromolecules 49:6655–6668
29. Jin S, Liu M, Chen S, Gao C (2008) Salt-induced micelle behavior of poly(sodium acrylate)-block-poly(*N*-isopropylacrylamide) by ATRP. Macromol Chem Phys 209:410–416
30. André X, Burkhardt M, Drechsler M, Lindner P, Gradzielski M, Müller AHE (2007) Schizophrenic micelles from a poly(Acrylic Acid)-*block*-poly(*N*,*N*-Diethylacrylamide) copolymer. Polym Mater Sci Eng 96:560–561
31. André X, Zhang M, Müller AHE (2005) Thermo- and pH-responsive micelles of poly(acrylic acid)-*block*-poly(*N*,*N*-diethylacrylamide). Macromol Rapid Commun 26:558–563
32. Yee MM, Tsubone M, Morita T, Yusa S-I, Nakashima K (2016) Fluorescence ON-OFF switching using micelle of stimuli-responsive double hydrophilic block copolymers: Nile red fluorescence in micelles of poly(acrylic acid-*b*-*N*-isopropylacrylamide). J Lumin 176:318–323
33. Barner-Kowollik C (2008) Handbook of RAFT polymerization. Wiley-VCH, Weinheim,
34. Yusa S, Endo T, Ito M (2009) Synthesis of thermo-responsive 4-arms star-shaped porphyrin-centered poly(*N,N*-diethylacrylamide) via reversible addition-fragmentation chain transfer (RAFT) radical polymerization. J Polym Sci A Polym Chem 47:6827–6838
35. Matsuoka H, Mouri E, Matsumoto K (2001) Nanostructure of polymer assemblies at air/water Interface by X-ray reflectometry. Rigaku J 18:54–67
36. Mouri E, Matsumoto K, Matsuoka H (2003) Effect of pH on the nanostructure of acidic amphiphilic Carbosilane/Methacrylic acid block copolymer monolayers at air/water interface. J Appl Crystallogr 36:722–726
37. Matsuoka H, Suetomi Y, Kaewsaiha P, Matsumoto K (2009) Nanostructure of poly(acrylic acid) brush and its transition in the amphiphilic Diblock copolymer monolayer on the water surface. Langmuir 25(24):13752–13762
38. Matsuoka H, Yamakawa Y, Ghosh A, Saruwatari Y (2015) Nanostructure and salt effect of Zwitterionic Carboxybetaine brush at the air/water interface. Langmuir 31:4827–4836
39. Matsuoka H, Uda K (2016) Nanostructure of poly(N-isopropylacrylamide) brush at the air/water Interface and its responsivity to temperature and salt. Langmuir 32(33):8383–8391
40. Matsuoka H, Ogura Y, Yamaoka H (1998) Effects of counterioin species on the dynamics of polystyrenesulfonate in aqueous solution as studied by dynamic light scattering. J Chem Phys 109(14):6125–6132
41. Zhang Y, Fyryk S, Bergbreiter DE, Cremer PS (2005) Specific ion effects on the water solubility of macromolecules: PNIPAM and the hofmeister series. J Am Chem Soc 127(41):14505–14510
42. Ghosh A, Yusa S, Matsuoka H, Saruwatari Y (2013) Effect of chain length and salt on the temperature-responsive cationic amphiphilic Diblock copolymer. J Chem Biol Interf 1(1):41–48
43. Weaire D, Hutzler S (1999) The physics of foams. Oxford University Press, Oxford,
44. Israelachvili J (1991) Intermolecular & surface forces, 2nd edn. Academic, San Diego,